Molecular simulation study of miscibility of ternary and quaternary InGaAlN alloys

Jhumpa Adhikari and David A. Kofke
Department of Chemical and Biological Engineering, University at Buffalo, The State University of New York, Buffalo, New York 14260-4200

(Received 23 December 2003; accepted 8 March 2004)

Molecular simulations are conducted to determine the limits of miscibility of a valence force field model for zinc-blende-structured $In_{1-x-y}Ga_xAl_yN$ semiconductor alloys. The transition matrix Monte Carlo method is used to calculate the free energy of the model alloys as a function of temperature and alloy composition (considering both x and y ranging from zero to unity). Analysis of the free-energy surface provides values for the upper critical solution temperature of the ternary alloys: InGaN (1550 K), InAlN (2700 K), and GaAlN (195 K). The miscibility envelope of the quaternary alloy is determined at 773 K and 1273 K. The excess properties of the mixtures are calculated, and it is found that the excess entropy is negligible, and the excess enthalpy is nearly independent of temperature. Consequently, regular-solution theory provides a good description of the thermodynamic properties of the alloys, and comparison of the simulation results with the phase behavior previously reported using regular-solution theory finds good agreement. Structural properties of the ternary compounds are examined in terms of the local compositions. For InGaN it is found (surprisingly) that there is a slight preference for In atoms to have Ga atoms rather than other In atoms as neighbors, in comparison to a random mixture. The two other ternary compounds exhibit the expected behavior, in which the (small) deviations from random mixing tend to favor segregation of like atoms. Among the ternaries, GaAlN is found to show the greatest deviations from random mixing. [DOI: 10.1063/1.1728317]

I. INTRODUCTION

AlN, GaN, and InN and their solutions are wide band gap semiconductors, which crystallize in both the cubic zinc blende structure as well as the hexagonal wurtzite structure. The ternary alloys InGaN, InAlN, and GaAlN and the quaternary alloy InGaAlN exhibit a wide range of band gap energies, varying with the composition and covering almost the entire visible spectrum while extending into the ultraviolet region. InGaN can be used in the manufacture of lasers and light-emitting diodes (Ref. 1) that can emit in the violet or blue wavelengths. However, the large lattice mismatch between the InN lattice and GaN lattice, which is of the order of 11%, causes difficulties in the growth of this alloy. InAlN alloys have a wide range of band gap energies that match almost the entire solar spectrum and can be used in the development of solar cells with 50% efficiency.[2,3] This compound also is difficult to grow and characterize owing to the large mismatch of the InN and AlN lattices. It has been observed experimentally[3,4] that, with the exception of GaAlN, the large lattice mismatches between the constituent binary compounds cause phase separation in the alloys through much of the composition range at the common growth temperatures. This behavior can have a great impact on the manufacture and performance of these materials.

Equilibrium thermodynamic phase behavior is more relevant to growth using metal-organic chemical vapor deposition as compared to molecular beam epitaxy, but regardless it is helpful to understand the stability of these systems with respect to demixing, even if they are not able to equilibrate. It is difficult to quantify the phase behavior experimentally, and consequently modeling studies have been applied to help to characterize it. Molecular simulation[5] is a good tool to apply for this purpose, but as of yet it has not been used to examine the phase and structural properties of these compounds. The present work aims to fill this void, and expands on our recent work focusing on miscibility in the InGaN system.[6]

The phase behavior is summarized in a miscibility diagram.[7] A key point on the diagram is the upper critical solution temperature (UCST), above which the solid solution is miscible in all proportions. Below this temperature, phase separation occurs such that over a temperature-dependent range of composition the stable system is one having two coexisting phases of different composition. Consequently there is a limit to the maximum amount of constituents that can be incorporated into each alloy while retaining its thermodynamic stability. It is useful to know the limits of stability for a given temperature. Also of interest are local compositions at various alloy compositions, which can also be determined from simulation. Local compositions describe the chemical environment around each atom. In the *random mixture*, the probability that a neighboring atom is of a particular type given simply by the bulk mole fraction of the components. Deviations from this behavior indicate composition inhomogeneities, which can have a disproportionate effect on electronic properties.

The approach taken in this work uses the empirical valence force field (VFF) model[8] as the interaction potential between constituent atoms, to which molecular simulation

TABLE I. Parameters for the valence force field model (Ref. 9).

System	d_0 (Å)	α (N/m)	β/α
AlN	4.38	86.53	0.1653
GaN	4.52	81.09	0.1500
InN	4.98	63.58	0.1266

methods are applied to calculate rigorously the limits of stability of the solid solutions, and their structural properties, as a function of temperature. We begin with a review of the VFF model and prior efforts to establish its miscibility behavior using approximate techniques.

A. Valence force field potential model

For III-V alloy systems, the lattice constants of the binary constituents are different, and when these constituents are mixed there arises a strain due to lattice mismatch. This microscopic strain energy is represented in the empirical VFF model. In this study, the VFF strain energy is taken as the interatomic potential between a central N atom and its four Al, In, and/or Ga neighbors in the cubic zinc blende structure. The VFF model is the sum of two-body and three-body contributions that take into consideration the bond stretching and bond bending, respectively,[8]

$$E_m = \frac{3}{8}\sum_{i=1}^{4} \alpha_i \frac{(d_i^2 - d_{i0}^2)^2}{d_{i0}^2} + \frac{6}{8}\sum_{i=1}^{4}\sum_{j=i+1}^{4} \frac{\beta_i+\beta_j}{2} \frac{(\mathbf{d}_i\cdot\mathbf{d}_j + d_{i0}d_{j0}/3)^2}{d_{i0}d_{j0}}, \quad (1)$$

where $\mathbf{d}_i$ is the vector (of magnitude d_i) between the central N atom and a corner atom in the tetrahedron, d_{i0} is the equilibrium bond length in the corresponding binary compound, α is the bond-stretching force constant, and β is the bond-bending force constant. For a perfect, undistorted InN, AlN, or GaN crystal, $E_m = 0$. Model constants for different components[9] are summarized in Table I.

B. Regular-solution theory

It is not a simple matter to establish the bulk-phase properties of a system that is specified in terms of a molecular model. No fully realistic system is completely solvable in this regard, so the development of statistical-thermodynamic models requires the application of an approximate treatment to the (already approximate) molecular model. One of the simplest such approaches for mixtures is the regular-solution theory, which was first applied to semiconductor systems by Ho and Stringfellow[10] and variations have subsequently been considered by others.[11] Regular-solution theory is a thermodynamic model in which the central approximation is the neglect of the excess entropy and volume of mixing.[7,12] It therefore equates the excess Gibbs free energy—which is needed to evaluate the miscibility behavior—to the excess enthalpy. The regular-solution model can be derived from the assumption of random mixing.

For the general quaternary compound $Ga_xAl_yIn_zN$ (such that $x+y+z=1$) the Gibbs free energy of mixing

$$\Delta G_M = \Delta H_M - T\Delta S_M = G - (xG_{GaN} + yG_{AlN} + zG_{InN}) \quad (2)$$

is approximated as follows:

$$\Delta G_M/N = \Omega_{GaAl}xy + \Omega_{GaIn}xz + \Omega_{AlIn}yz + kT(x\ln x + y\ln y + z\ln z), \quad (3)$$

where k is Boltzmann's constant, T is the temperature, N is the number of atoms, and Ω_{AB} is the regular-solution model interaction parameter for the ABN ternary. In Eq. (2), G is the Gibbs energy of the mixture, and G_A is the value for the pure component AN. In Eq. (3), the first three terms are the enthalpy of mixing ΔH_M from the regular-solution model and the last term is the entropy of mixing ΔS_M assuming a completely random distribution of Ga, Al, and In atoms. Models for the three ternaries are obtained as special cases in which one of the mole fractions (xyz) is zero.

Depending on the nature of the system, the excess enthalpy can be estimated in a variety of ways. In the approach taken by Ho and Stringfellow,[9,10] it is given in terms of the zero-temperature strain energy associated with the replacement of one atom in a pure nitride crystal with a different, solute atom. In response to the substitution, atoms as far as the sixth nearest neighbor are allowed to relax to an energy minimum. This energy will necessarily be larger than the energy of the perfect crystal (which is zero for this model), and the difference is used for the calculation of the interaction parameter Ω (e.g., Ω_{GaAl} is obtained by changing a Ga atom to Al in an otherwise pure GaN crystal). This treatment is appropriate only for very dilute alloys, and accordingly Ho and Stringfellow consider the strain energies for the two infinitely dilute limits, and average these values to arrive at a value of Ω for the system.

There are three approximations involved in the modeling undertaken by Ho and Stringfellow: first is the VFF molecular model to characterize lattice strain for different compositions; second is the evaluation of the excess enthalpy in terms of the zero-temperature strain energy; and third is the neglect of the excess entropy and volume in describing the mixtures (regular solution). The present study aims to provide information that permits these approximations to be evaluated independently, so that the strengths and weaknesses of the Ho-Stringfellow approach can be identified. The Ho-Stringfellow study examined alloys in the cubic zinc blende structure, and to allow a proper comparison of their work we examine systems with this symmetry too. Wurtzite is the more common form for these materials, but at the level of detail afforded by the VFF model, it is not expected that the behavior of interest here will be greatly different for the two morphologies. In the following section we describe the simulation methods employed in this work, and in Sec. III we present and discuss the results. Section IV provides concluding remarks.

II. SIMULATION METHODS

Determining of the miscibility behavior of the solid solution by molecular simulation is accomplished by evaluating the mixture free energy as a function of composition. The advantage of applying molecular simulation for this task is that it is capable of providing essentially exact values of the free energy for the given molecular model. Nevertheless, free-energy measurement by molecular simulation can be difficult, and we have considered several approaches to this problem. We have found it effective and feasible to map the entire free-energy surface over all compositions for several temperatures, and from this we can apply a minimization criterion to locate the UCST and the miscibility limits of solutions at temperatures below it. We have focused in addition on the limits of infinite dilution, and have applied additional methods to characterize the free energy in these regimes.

A. Transition matrix Monte Carlo method

The primary technique used in our calculations is the transition matrix Monte Carlo (TMMC) method[13–15] in the semigrand isothermal-isobaric ensemble.[16,17] This ensemble is formulated to permit fluctuations in composition at fixed number of atoms N; its partition function Y is a function of T, P, ξ_1, and ξ_2, where ξ_i is the fugacity fraction of component i[17,18] and P is the pressure. In this ensemble, the probability to observe the system to have a given composition is (at a specified T and P)

$$\Pi(N_1,N_2;\xi_1\xi_2,N)\propto\Delta(N_1,N_2;N)(1-\xi_1-\xi_2)^{N-N_1-N_2}\times\xi_1^{N_1}\xi_2^{N_2}/Y(\xi_1,\xi_2), \tag{4}$$

where $\Delta(N_1,N_2;N)=\exp[-\beta G(N_1,N_2;N)]$ is the (canonical) isothermal-isobaric partition function, related to the Gibbs free energy G of the mixture, and which serves as the density of states for the semigrand ensemble; also $\beta=1/kT$. The TMMC method provides information that permits evaluation of the probability distribution Π, which then provides the Gibbs free energy of the mixture via these formulas.

In the TMMC method,[13–15] as the name suggests, the raw data are the elements of a transition matrix, each element describing the probability that a semigrand Monte Carlo (MC) trial will move the system from one composition to another. The limiting distribution that corresponds to the measured transition-probability matrix is the density of states. TMMC methods seem to have some advantages over visited-state techniques for evaluation of the density of states. The relative merits of these approaches have been discussed in detail elsewhere.[14,15,19] We briefly review the steps involved in the application of the TMMC method for the system of interest here.

We define a macrostate S of our system in terms of the number of atoms $S=\{N_{Ga},N_{Al},N_{In}\}$, and we recognize that each macrostate is consistent with a large number of possible microstates $s(\mathbf{r}^N,S)$, which are further distinguished by the detailed arrangement (coordinates $\mathbf{r}^N$) of the atoms in the system volume. Any MC trial $s\rightarrow s'$ results in the attempted transition between two macrostates $S\rightarrow S'$, including the case in which $S'=S$ (i.e., the case in which the mixture composition does not change). A given trial is accepted with probability $a(s\rightarrow s')=\min[1,\pi(s')/\pi(s)]$, where $\pi(s)$ is the probability to observe microstate s in the semigrand ensemble.[5,17] In the TMMC procedure, a collection matrix C is updated after each step (regardless of acceptance) as follows: $C(S\rightarrow S')=C(S\rightarrow S')+a(s\rightarrow s')$ and $C(S\rightarrow S)=C(S\rightarrow S)+1-a(s\rightarrow s')$. The macrostate transition probabilities are obtained at any time by normalizing the collection matrix with respect to all target states. We attempt only moves in which one atom (at most) changes its species identity, (causing one of the N_i to be incremented by 1 while another is decremented). This feature simplifies the process of solving for the limiting distribution $\Pi(S)$.[15] Once it is determined, the Gibbs free energy as a function of composition can be evaluated using Eq. (4). For simulations of the larger systems we found it helpful to restrict the composition to "windows" of width $\Delta N=32$, limiting the range of values that the number of atoms of a species can fluctuate. Data collected within each window can be easily combined with other window data to get the full transition-probability matrix.

MC simulations were conducted in the semigrand isothermal-isobaric ensemble where the trial moves include atom displacement trials, volume change trials, and identity change trials with the frequency ratio $N:1:N$. Equal fugacity fractions were used for all species. The ternary systems were simulated using 216 particles (108 nitrogen and 108 Ga/Al/In). Each simulation was conducted for 15×10^6 MC trials, and the TMMC weights (applied to promote even sampling of the compositions) were updated every 10^6 steps. Finite-size effects were assessed by doing simulations for a 512-particle InGaN system at temperatures of 600 K, 1000 K, and 1600 K. These simulations were carried out for 30×10^6 steps, and windowing was applied for the TMMC method. No appreciable size effects were observed and hence, for the other two alloys, viz., AlInN and GaAlN, only simulations with 216 particles were conducted.

For the quaternary alloy $Ga_xAl_yIn_zN$, the simulations were performed for a 512-particle system with 30×10^6 MC steps being used to determine the extensive Gibbs free energy as a function of composition. Windows were used in each simulation run for the TMMC calculations. The MC trials considered here included volume change trials, trial particle displacements, identity change trials in which In and Ga atoms were allowed to switch identities while keeping the Al content unchanged, and a trial to swap positions of any pair of the three group III elements (In, Ga, Al). Separate runs were performed for Al mole fraction y constant at regular intervals of 0.1 starting from $y=0.0$ ($Ga_xIn_{1-x}N$) to $y=0.9$. Free energies for Al compositions between these values were evaluated via interpolation of the excess Gibbs free energy subsequently derived from the simulation data. Coexistence compositions were determined by minimizing the Gibbs free energy of a composite system subject to the constraint of a fixed overall compositions. Studies were performed for two temperatures: 773 K and 1273 K.

B. Infinite-dilution behavior

We pay particular interest to the behavior at infinite dilution, as this is the condition for which the Ho-Stringfellow study obtained the regular-solution mixing enthalpy via the strain energy. We wish to consider the dependence of this quantity on the temperature, to ascertain whether it is reasonable to apply the zero-temperature (energy minimized) strain energy for this purpose. We examined the temperature-dependent infinite-dilution free energy of mixing as a function of temperature, from 0 K to the UCST. This information can be obtained from the TMMC data, but we found that the data for the In-rich systems was somewhat noisy, particularly at low temperatures, and that alternative methods could be applied to obtain better results for this purpose.

One approach that we applied is simple free-energy perturbation (FEP).[5] In this method, we simulate pure systems (no solute, e.g., InN) and ''rich'' systems (with one solute atom, e.g., substituting a Ga atom for one of the In atoms) and evaluate their difference in Gibbs free energy by perturbing into each other during the course of an isothermal-isobaric MC simulation. Direct perturbation gives a result that is no better than the TMMC calculation, so we applied the overlap-sampling staging method to improve the quality of the results.[19,20] Briefly, if we designate the pure and rich systems by 0 and 1, respectively, we perform perturbations into an intermediate system, designated *W*, with energy defined as the maximum of the energies of the two systems of interest for a given configuration: $U_W(\mathbf{r}^N) = \max[U_0(\mathbf{r}^N), U_1(\mathbf{r}^N)]$. We perform separate simulations of the 0 and 1 systems, and evaluate the desired free-energy difference in terms of the two FEP ensemble averages, thus

$$e^{-\beta(G_1-G_0)} = \frac{\langle e^{-\beta(U_w-U_0)}\rangle_0}{\langle e^{-\beta(U_w-U_1)}\rangle_1}. \tag{5}$$

We applied thermodynamic integration (TI) in temperature as the second approach to describe the infinite-dilution behavior. The basic formula is

$$[\beta\Delta G](\beta) = [\beta\Delta G](\beta_0) + \int_0^\beta [\langle \beta H\rangle_1(\hat{\beta}) - \langle \beta H\rangle_0(\hat{\beta})]d\hat{\beta}. \tag{6}$$

That is, the free-energy difference at one temperature (designated by the reciprocal temperature β) is given in terms of its value at another temperature β_0, plus an integral over temperature involving the ensemble-average enthalpy of the rich system $\langle \beta H\rangle_1$ minus that of the pure system, each evaluated at the (reciprocal) temperature $\hat{\beta}$. The rich and pure ensemble-average enthalpies are measured in separate simulations of the respective systems, so unlike the TMMC and FEP methods, this approach requires no perturbation involving an identity change of an atom. We take the reference free-energy difference (at β_0) to be that measured by the TMMC and FEP simulations at the highest temperature to which they are applied, where precise results can be obtained by these methods. Integration can be extended to near-zero temperature, allowing for a good comparison with the Ho-Stringfellow energy-minimization results.

The results from either method give the infinite-dilution Gibbs free energy for solvation of atom *A* in the pure *B* nitride, $\Delta G^\infty_{B\to A}$, or the atom *B* in the pure *A* nitride, $\Delta G^\infty_{A\to B}$. Then, to the extent that Eq. (3) applies, the infinite-dilution solvation free energy is sufficient to determine Ω for the *AB* pair, applying either limiting condition. The parameter relates to the solvation free energy as follows:

$$\Omega_{AB} = \begin{cases} \Delta G^\infty_{A\to B} + (g^o_{\mathrm{AN}} - g^o_{\mathrm{BN}}) & B \text{ dilute} \\ \Delta G^\infty_{B\to A} + (g^o_{\mathrm{BN}} - g^o_{\mathrm{AN}}) & A \text{ dilute,} \end{cases} \tag{7}$$

where g^o_{AN} and g^o_{BN} are the molar Gibbs free energies of the pure AN and BN systems. This is the generalization to finite temperatures of the Ho-Stringfellow approach to evaluate Ω using the zero-temperature strain energy. Of course, the real mixture will deviate from Eq. (3) to some extent, and this will cause the two limiting cases to yield different values for Ω, as observed also by Ho and Stringfellow.

III. RESULTS AND DISCUSSION

A. Ga_xIn_zN

1. Phase diagram

The free energy and phase behavior of the Ga_xIn_zN ($y=0$) system, as given by the methods described here, was recently reported.[6] The miscibility diagram shows a UCST of 1550 K which is slightly higher than that determined by Ho and Stringfellow. One expects the regular-solution treatment to overestimate the UCST, and the fact that it does not is explained by a compensating inaccuracy in using the $T=0$ K values of the infinite-dilution free energy of mixing. The study also found that the excess entropy is practically zero and that the excess enthalpy is effectively independent of temperature.

2. Local composition

There are 12 nearest In or Ga neighbors for every group III atom in the zinc blende structure. Thus for a completely random mixture (such as that assumed in the derivation of regular-solution theory) of the Ga_xIn_zN alloy, the number of nearest-neighbor In atoms surrounding a central In atom should be $12z$. One would expect that at lower temperatures, below the UCST, the tendency to phase separate would give rise to some nonrandomness in the local compositions, such that clusters of pure InN regions and pure GaN regions would be observed. The presence of such clusters would be important practically, as they would affect the electronic properties of the material. Quantitatively, the effect of clustering would cause the average number of nearest-neighbor In atoms surrounding a core In atom to be greater than that for a random mixture. Surprisingly, our simulation results indicate the opposite trend. Data for three compositions (viz., $x=0.25$, $x=0.50$, $x=0.75$) and three different system sizes (216, 512, and 1000 particles) are summarized in Fig. 1, and in more detail in Fig. 2(a). The latter figure shows the histogram of neighbor counts for all In atoms in the system. At an equimolar composition of $In_{0.5}Ga_{0.5}N$ (for example), in a completely random mixture this histogram should have a peak at 6, but simulation results show the peak at 5.6. Figure

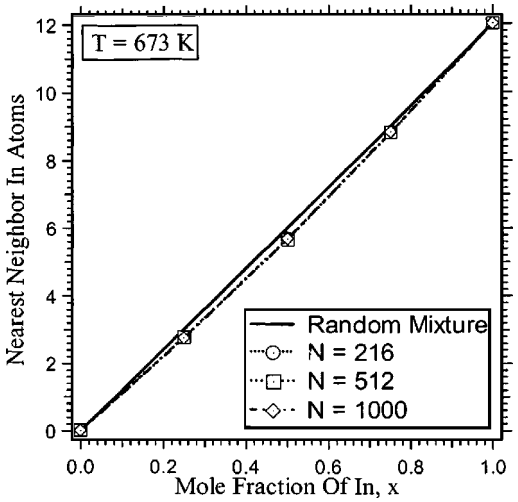

FIG. 1. The nearest neighbors of In atoms around a central In atom as a function of composition in the $In_xGa_{1-x}N$ alloy for different simulation system sizes. The random mixture line is $12x$, which holds to the extent that regular-solution theory is valid.

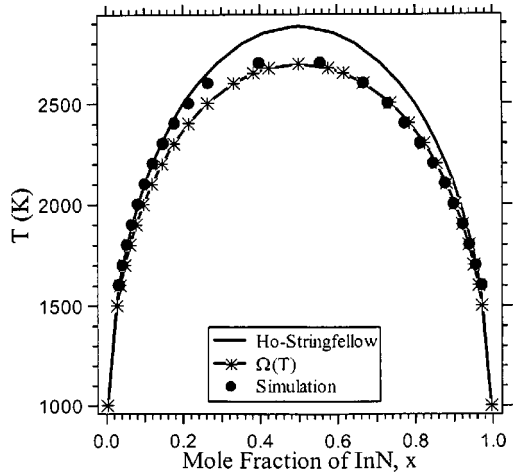

FIG. 3. Miscibility diagram for $In_xAl_{1-x}N$ alloy. The Ho-Stringfellow curve is regular-solution theory using $\Omega = 11.45$ kcal/mol. The curve labeled $\Omega(T)$ is regular-solution theory with temperature dependent Ω given as an average of the infinite-dilution values reported in Fig. 4. The circles describe results of TMMC calculations for a 216-particle system.

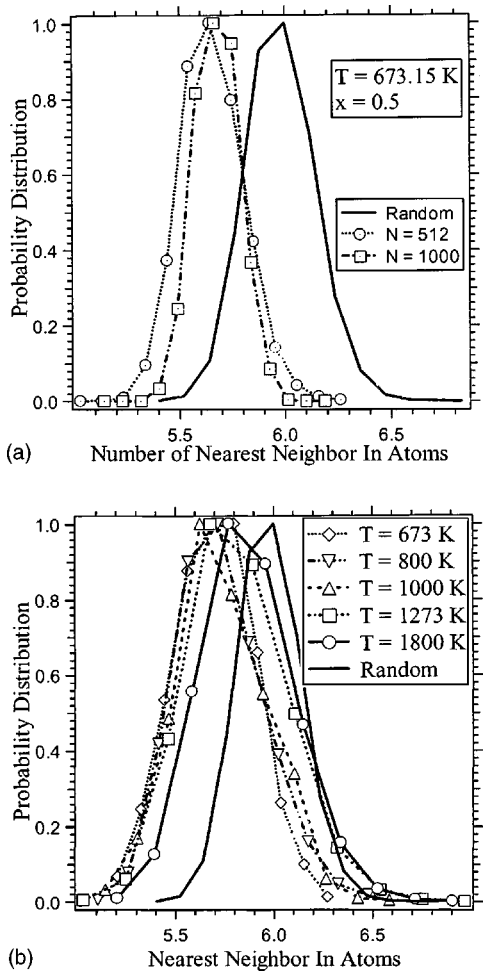

FIG. 2. Histogram of count of In atoms in (any of 12) nearest-neighbor positions about a central In atom in the $In_xGa_{1-x}N$ alloy with $x = 0.5$. Curve labeled "random" describes simulation results for an equimolar ideal alloy (all atoms having identical interactions; random mixture). (a) Simulation system-size dependence at $T = 673.15$ K; (b) temperature dependence for system of 256 atoms.

2(b) further shows the migration of the peak with temperature. As the temperature increases from 673 K to 1273 K, we notice that the distribution remains centered around the same value. However, for a temperature of 1800 K, which is higher than the critical temperature of 1550 K, the probability distribution peaks closer to the random mixture value of 6.0.

The simulation results indicate that in all cases there is a small but significant deviation towards a *lower* In-In local mole fraction, and that this behavior is not caused by a spurious finite-size effect. Perhaps the result is an anomalous feature of the molecular model; regardless it is an unexpected phenomenon that could benefit from further study.

Additional details, including analysis of the volume of mixing (which is found to be nearly ideal, in line with Vegard's law) and bond lengths, are presented elsewhere.[21]

B. Al_yIn_zN

In this alloy, the lattice constants of the pure binary constituents are more than 12% apart indicating that this alloy will be immiscible up to a considerably high temperature; this expectation is borne out by the results of the simulations.

1. Phase diagram

The miscibility diagram determined by TMMC simulations is shown in Fig. 3 which also includes the Ho and Stringfellow phase diagram, which was determined using $\Omega = 11.45$ kcal/mol. The UCST as determined from Ho and Stringfellow regular-solution calculations gives 2882 K, which unlike that for the InGaN system, is as expected above the simulation UCST of 2700 K. Regular-solution theory with a temperature-dependent interaction parameter yields a UCST in agreement with the simulation result, again indicating that the theory is valid for this system. From Fig. 4 showing the Ω calculation, we can observe that the TMMC, FEP, and TI calculations are in good mutual agreement. Moreover their extrapolation to $T = 0$ K appears to agree with the Ho and Stringfellow value of Ω for InN as solute,

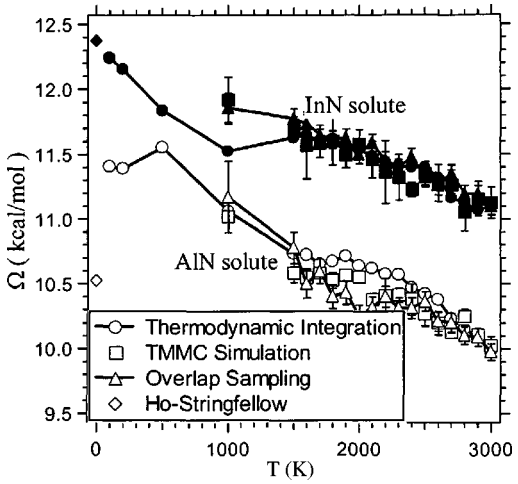

FIG. 4. Regular-solution interaction parameter for the $In_xAl_{1-x}N$ alloy, determined by calculation of the Gibbs free energy of solvation at infinite dilution. The filled markers indicate values for InN as a solute in otherwise pure AlN, while the open markers are the complementary case of AlN dilute in InN. Values are computed using the overlap sampling [Eq. (5)] and thermodynamic integration [Eq. (6)] methods, as indicated. The Ho and Stringfellow (see Ref. 9) interaction parameters are also shown in the figure at $T=0$. Additionally, results from the application of the TMMC method at infinite dilution are presented.

but the AlN-solute extrapolation shows considerable disagreement, as seen in the InGaN case.[6] The excess properties are presented in Fig. 5, where we observe the same trends seen in the InGaN system: the excess molar entropy is approximately zero and the excess enthalpy is independent of temperature, both in support of regular-solution theory.

2. Local composition

For this system the local compositions behave in a way consistent with expectations. The probability distribution of neighboring In atoms around a core In atom in this alloy at 673 K and $z=0.25$, 0.5, 0.75 indicates that there is a greater concentration of In atoms around In atoms than would be found in a random alloy. This behavior fits with the inclination of the system at this temperature to form separate InN and AlN phases. Results are presented in Fig. 6.

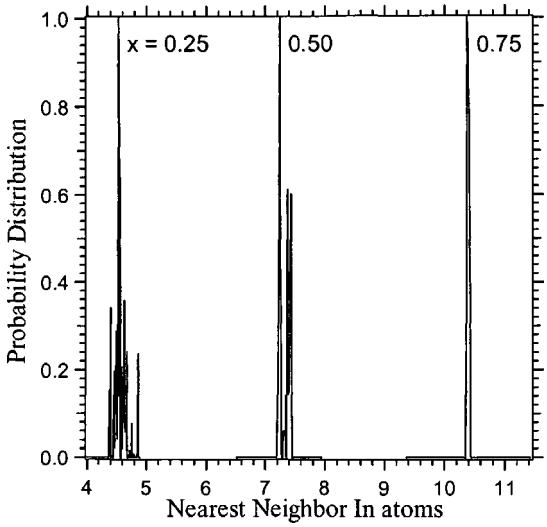

FIG. 6. Histogram of count of In atoms in (any of 12) nearest-neighbor positions about a central In atom in the $In_xAl_{1-x}N$ alloy at 673 K and three compositions x, as indicated. For a random distribution, the peaks should be at 3, 6, and 9 for $x=0.25$, 0.5, and 0.75, respectively.

C. Ga_xAl_yN

The lattice constant for pure GaN is 4.52 Å and that for pure AlN is 4.38 Å. Hence, the lattice mismatch in this alloy is only about 3%, which means that this alloy is miscible at temperatures above room temperature. The simulation results in this study agree with this expectation.

1. Phase diagram

TMMC simulation results for the miscibility diagram are shown in Fig. 7, including the Ho and Stringfellow result,

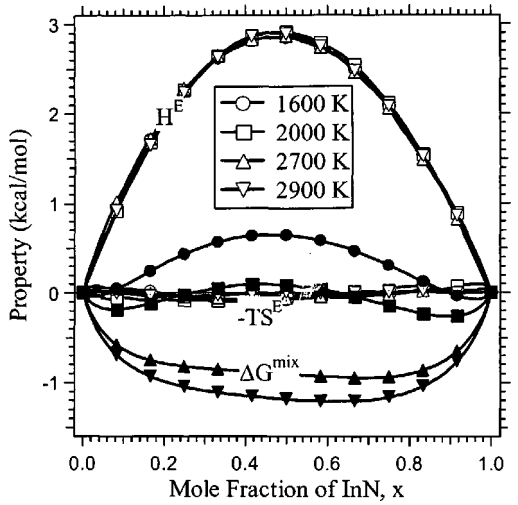

FIG. 5. Mixing properties as a function of composition at different temperatures for the $In_xAl_{1-x}N$ alloy. The molar mixing Gibbs free energy is represented by the filled markers, while the open symbols describe the excess enthalpy H^E and (minus) the excess entropy times the temperature $(-TS^E)$, as indicated.

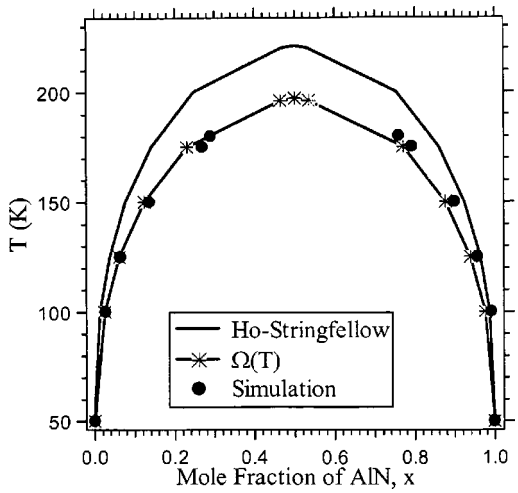

FIG. 7. Miscibility diagram for $Al_xGa_{1-x}N$ alloy. The Ho-Stringfellow curve is regular-solution theory using $\Omega=0.88$ kcal/mol. The curve labeled $\Omega(T)$ is regular-solution theory with temperature dependent Ω given as an average of the infinite-dilution values reported in Fig. 8. The circles describe results of TMMC calculations for a 216-particle system.

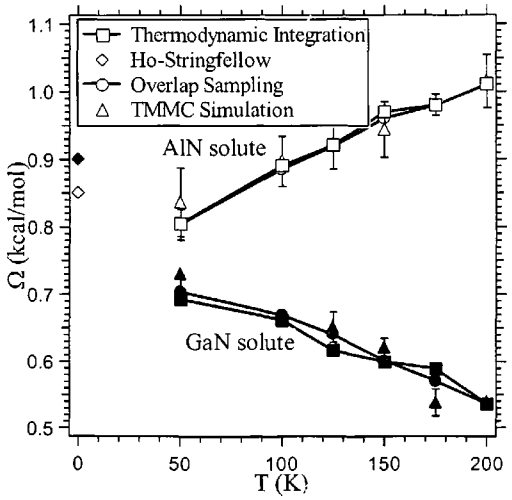

FIG. 8. Regular-solution interaction parameter for the $Al_xGa_{1-x}N$ alloy. The filled markers indicate values for GaN as a solute in otherwise pure AlN, while the open markers are the complementary case of AlN dilute in GaN. Values are computed using the overlap sampling [Eq. (5)] and thermodynamic integration [Eq. (6)] methods, as indicated. The Ho and Stringfellow (see Ref. 9) interaction parameters are also shown in the figure at $T=0$. Additionally, results from the application of the TMMC method at infinite dilution are presented.

which uses a constant Ω_{GaAl} of 0.88 kcal/mol. The UCST as determined from regular-solution calculations is 221 K whereas the temperature-dependent interaction parameter results in UCST of 197 K, which is about equal to the TMMC simulation UCST of ≈195 K. From Fig. 8, showing the Ω calculation, we can observe that the three methods used to characterize the infinite-dilution behavior are once again in good agreement. The $T=0$ intercept again shows some discrepancy with Ho and Stringfellow result, this time yielding interaction parameters lower than those previously reported. In Fig. 9, we see again that the excess molar entropy is approximately zero, although in this case there is a noticeable deviation from zero. The deviation is still much smaller than the excess enthalpy, and consequently it has little influence on the mixture behavior.

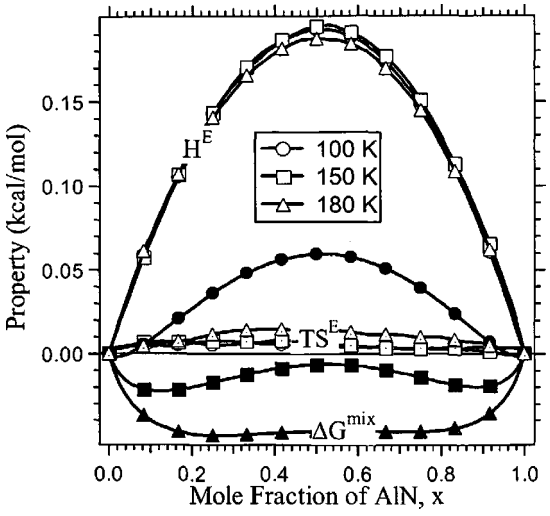

FIG. 9. Mixing properties as a function of composition at different temperatures for the $Al_xGa_{1-x}N$ alloy. The molar mixing Gibbs free energy is represented by the filled markers, while the open symbols describe the excess enthalpy H^E and (minus) the excess entropy times the temperature $(-TS^E)$, as indicated.

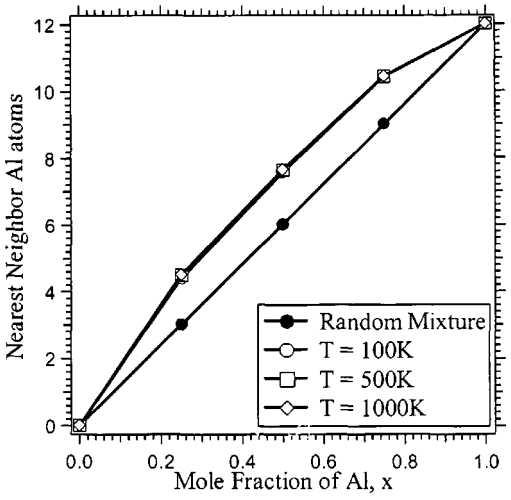

FIG. 10. The number of nearest neighbors of Al atoms around a central Al atom as a function of composition in the $Al_xGa_{1-x}N$ alloy for different simulation system sizes. The random mixture line is $12x$, which holds to the extent that regular-solution theory is valid.

2. Local composition

Figure 10 shows the nearest neighbors of Al atoms around a core Al atom as a function of composition in the alloy, and the data show a significant deviation from random mixing at all three temperatures studied, even though 100 K is lower than UCST and the other two temperatures (500 K and 1000 K) are much higher than the UCST. The deviation from random mixing is really quite large, such that for the equimolar system each Al atom is, on average, surrounded by two additional Al atoms at the expense of the Ga atoms. This indicates short range ordering which contradicts the regular-solution assumption of randomly mixed alloys, and is consistent with the nonzero excess entropy observed in Fig. 9. It is rather surprising that this mixture, which among the ones studied has the greatest lattice match, also shows the greatest deviation from random mixing. An explanation might lie in the fact that we are studying this system at temperatures generally lower than examined in the other systems (because the UCST is lower), but even when going to 1000 K we still observe the same degree of deviation from the random case. Indeed, over the range studied, there seems to be no effect of temperature at all.

D. $Ga_xAl_yIn_zN$

We are now ready to turn to the quaternary alloy, but first let us consider the consistency of the ternaries when taken together. If we arbitrarily assign the free energy of pure GaN to be zero, $g_{GaN}=0$ kcal/mol at 1273 K, the TMMC calculations performed for InGaN can be used to determine the relative free energy of pure InN, and from this we get $g_{InN}=-101.44$ kcal/mol. This value used in conjunction with the TMMC data for GaAlN then permit us to determine $g_{AlN}=34.09$ kcal/mol. We can then complete the cycle with

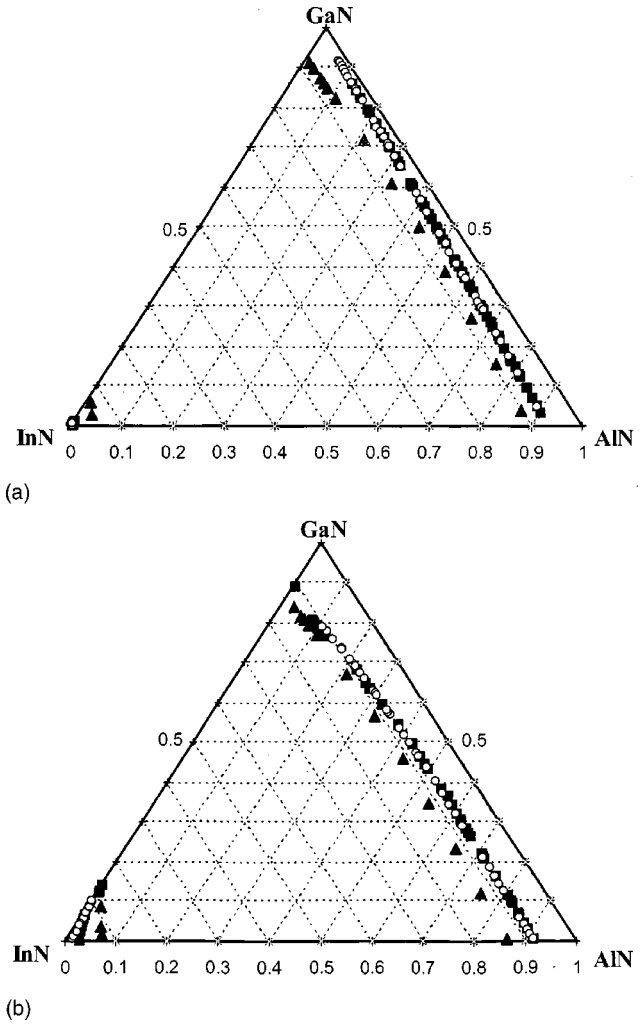

FIG. 11. Ternary miscibility diagram for $In_{1-x-y}Ga_xAl_yN$. The filled triangles are the loci of the spinodal and the open circles are the binodal isotherm points as given by the regular-solution theory. The filled squares are the simulation results for the binodal. (a) $T=773$ K; (b) 1273 K.

the data for InAlN, and upon returning to pure GaN we have $g_{\mathrm{GaN}}=0.04$ kcal/mol. Clearly, this is close to the value of 0 kcal/mol originally assigned to this compound, and the agreement indicates that the quality of the data for the respective ternaries is quite good.

As described above, we computed the free energy of the quaternary compound by performing TMMC calculations along a path of constant Al fraction, performing changes that swap the identities of the In and Ga atoms. We did this for 0.1 increments in y, from 0.1 to 0.9. The Gibbs free energy of mixing thus determined as a function of (x, y), we minimize it to get the ternary phase diagram shown in Fig. 11 for two temperatures 773 K [Fig. 11(a)] and 1273 K [Fig. 11(b)]. Also shown are the regular-solution binodal and the spinodal isotherms determined using the interaction parameters determined in the ternary-compound studies. Similar regular-solution calculations for this quaternary system (but in the wurtzite structure) have previously been reported by Matsuoka.[22] The binodal isotherms at both temperatures show excellent agreement with the simulation data, with the higher-temperature isotherm just slightly displaced from the regular-solution result. It is notable that the interaction parameters for the ternary compounds succeed in describing the phase behavior of the full quaternary.

Finally, we note another point of consistency in the simulation data. The simulations of the quaternary system begin with free energies of the GaAlN ternary, and proceed at constant Al content (y) until reaching the InAlN ternary. The result is a free energy profile for InAlN that is obtained independent of the data described in Sec. III B. Comparison of these free-energy profiles (not shown) finds that they are in agreement.

IV. CONCLUSIONS

The application of regular-solution theory to InGaAlN alloys has not previously been tested, and this work shows that it is a good approximation for all the ternary and quaternary alloys studied here. This conclusion is most significantly borne out by the approximately zero values for the molar excess entropies, as well as by the good description that regular-solution theory provides for the phase behavior in comparison to simulation. Local compositions exhibit behaviors that are difficult to explain. Slight desegregation is observed in the InGaN ternary, while the other ternaries tend toward aggregation of like atoms. The effect is greatest in GaAlN, the system with the least lattice mismatch.

ACKNOWLEDGMENTS

This work is supported by the U.S. Department of Energy, Office of Basic Energy Sciences. Computing resources have been provided by the University at Buffalo Center for Computational Research. We are grateful to Professor Alex Cartwright for helpful discussions, and for stimulating our interest in this topic.

[1] S. Nakamura, M. Senoh, N. Iwasa, and S. Nagahama, Jpn. J. Appl. Phys., Part 2 **34**, L797 (1995).
[2] S. N. Mohammad, A. Salvador, and H. Morkoc, Proc. IEEE **83**, 1306 (1995); J. Wu, W. Walukiewicz, K. M. Yu, J. W. Ager III, E. E. Haller, H. Lu, W. J. Schaff, Y. Saito, and Y. Nanishi, Appl. Phys. Lett. **80**, 3967 (2002).
[3] Y. Narukawa, Y. Kawakami, M. Funato, S. Fujita, S. Fujita, and S. Nakamura, Appl. Phys. Lett. **70**, 981 (1997).
[4] K. Osamura, S. Naka, and Y. Murakami, J. Appl. Phys. **46**, 3432 (1975); T. Matsuoka, N. Yoshimoto, T. Sasaki, and A. Katsui, J. Electron. Mater. **21**, 157 (1992); M. Shimizu, K. Hiramatsu, and N. Sawaki, J. Cryst. Growth **145**, 209 (1994); S. Chichibu, T. Azuhata, T. Sota, and S. Nakamura, Appl. Phys. Lett. **70**, 2822 (1997); N. A. El-Masry, E. L. Piner, S. X. Liu, and S. M. Bedair, *ibid.* **72**, 40 (1998); D. Doppalapudi, S. N. Basu, K. F. Ludwig, and T. D. Moustakas, J. Appl. Phys. **84**, 1389 (1998); M. D. McCluskey, L. T. Romano, B. S. Krusor, D. P. Bour, N. M. Johnson, and S. Brennan, Appl. Phys. Lett. **72**, 1730 (1998); K. P. O'Donnell, R. W. Martin, and P. G. Middleton, Phys. Rev. Lett. **82**, 237 (1999); V. Lemos, E. Silveira, J. R. Leite, A. Tabata, R. Trentin, L. M. R. Scolfaro, T. Frey, D. J. As, D. Schikora, and K. Lischka, *ibid.* **84**, 3666 (2000).
[5] D. Frenkel and B. Smit, *Understanding Molecular Simulation: From Algorithms to Applications*, 2nd ed. (Academic Press, New York, 2002).
[6] J. Adhikari and D. A. Kofke, J. Appl. Phys. **95**, 4500 (2004).
[7] J. M. Prausnitz, R. N. Lichtenthaler, and E. G. de Azevedo, *Molecular Thermodynamics of Fluid-Phase Equilibria* (Prentice-Hall, Englewood Cliffs, NJ, 1986).
[8] R. M. Martin, Phys. Rev. B **1**, 4005 (1970); P. N. Keating, Phys. Rev. **145**, 637 (1966).
[9] I.-H. Ho and G. B. Stringfellow, J. Cryst. Growth **178**, 1 (1997).
[10] I.-H. Ho and G. B. Stringfellow, Appl. Phys. Lett. **69**, 2701 (1996).

[11] T. Saito and Y. Arakawa, Phys. Rev. B **60**, 1701 (1999); T. Takayama, M. Yuri, K. Itoh, T. Baba, and J. S. Harris, J. Appl. Phys. **88**, 1104 (2000); Toru Takayama, Yuri Masaaki, Itoh Kunio, and S. J. Harris, Jr., *ibid.* **90**, 2358 (2001).
[12] G. B. Stringfellow, *Organometallic Vapor-phase Expitaxy: Theory and Practice* (Academic Press, New York, 1989).
[13] J.-S. Wang, T. K. Tay, and R. H. Swendsen, Phys. Rev. Lett. **82**, 476 (1999); J.-S. Wang and R. H. Swendsen, J. Stat. Phys. **106**, 245 (2002).
[14] M. Fitzgerald, R. R. Picard, and R. N. Silver, Europhys. Lett. **46**, 282 (1999); J. Stat. Phys. **98**, 321 (2000).
[15] J. R. Errington, J. Chem. Phys. **118**, 9915 (2003).
[16] J. G. Briano and E. D. Glandt, J. Chem. Phys. **80**, 3336 (1984).
[17] D. A. Kofke, Adv. Chem. Phys. **105**, 405 (1999).
[18] M. Mehta and D. A. Kofke, Chem. Eng. Sci. **49**, 2633 (1994).
[19] D. A. Kofke, Mol. Phys. (to be published).
[20] N. D. Lu, J. K. Singh, and D. A. Kofke, J. Chem. Phys. **118**, 2977 (2003).
[21] J. Adhikari, Ph.D. thesis, University at Buffalo, The State University of New York, 2003.
[22] T. Matsuoka, Appl. Phys. Lett. **71**, 105 (1997); MRS Internet J. Nitride Semicond. Res. **3**, 1 (1998).